Physics requirements for the VUV survey spectrometer intended for the divertor radiation monitoring on JT-60SA

M. Valisa[1], W Biel[2], F. Bombarda[3], L. Carraro[1], M. Chernyshova[4], I. Coffey[5], T. Czarski[4], S. Davis[6], A. Fassina[1], T. Fornal[4], L. Gabellieri[3], E. Kowalska-Strzęciwilk[4], I. Książek[7], K. Lawson[5], K. Malinowski[1], M. O'Mullane[8], T. Nakano[9], N. Oyama[9], A. Romano[3], M.E. Puiatti[1], S. Scully[5], S. Soare[10] and C. Sozzi[11]

[1]Consorzio RFX, 35127 Padova, Italy; [2]Institut für Plasmaphysik, Forschungszentrum Jülich Gmbh, D-52425 Jülich, Germany; [3]ENEA, Fusion and Nuclear Safety Department, C. R. Frascati, Via E. Fermi 45, 00044 Frascati (Roma), Italy; [4]Institute of Plasma Physics and Laser Microfusion, Warsaw, Poland; [5]CCFE, Culham Science Centre, Abingdon, OX14 3DB, UK; [6]Fusion for Energy, Garching, Germany; [7]Institute of Physics, Opole University, Opole, Poland; [8]University of Strathclyde, Glasgow, UK; [9]National Institutes for Quantum and Radiological Science and Technology (QST), Naka, Japan; [10]Universitatea "Lucian Blaga", Sibiu 55002, Romania, [11]CNR, Istituto di Fisica del Plasma, Milano, Italy

1. Introduction

The mission of JT-60SA is to contribute to the early realization of fusion energy by supporting the exploitation of ITER and by complementing ITER in resolving key physics and engineering issues for DEMO reactors [1]. Among a spectrum of options, JT-60SA will pursue fully non-inductive steady-state operations at high plasma pressure, exceeding the no-wall ideal MHD stability limits. High-β steady-state operations assisted by integrated plasma control systems will be firstly achieved with carbon plasma facing components (PFCs). In the later phase the divertor target and the first wall will be fully replaced by tungsten based PFC.

For the safe operation of the device, a survey spectrometer observing the plasma from an equatorial port is foreseen to monitor light impurities such as carbon and oxygen, metal impurities and extrinsic. A second survey spectrometer, to be designed and procured within the EUROfusion-QST collaboration, positioned on an upper port with a vertical line of sight, will complement the monitoring activity of the first system by measuring the relative contribution of the various impurities to the radiation losses in the divertor region and by studying the physics of the plasma-divertor detachment mechanism.

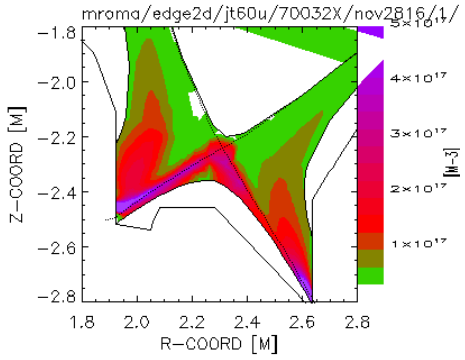

Fig. 1. Simulation of the 2D distribution of the C^{3+} population in the divertor, showing the complex topology of its spatial distribution.

2. Main scientific objectives

The divertor is the region where the hot magnetically confined plasma interacts with the surrounding structures. In order to master the power exhaust and in particular the heat load on to the divertor plates it is essential to know the radiation losses associated to the intrinsic impurities as well of the gases deliberately injected to enhance the radiative component of the power outflow.

Detailed spectroscopic investigations are required to understand the impurity behaviour and in the divertor region such an exercise is further hampered by the complex two dimensional structure of the magnetic configuration. A prediction of the 2D spatial distribution of C^{3+} is given in Fig. 1 for one sample JT-60SA scenario as it results from an EDGE2D simulation [2]. In the vicinity of the detachment phase a MARFE can develop around the X point of the configuration, characterized by a strong toroidally symmetric radiating pattern, cool and dense [3]. In other words, the topological complexity of the radiation pattern entails that the VUV divertor spectrometer should have imaging capabilities in order to at least resolve inner leg, outer leg and X-point region of the divertor.

Among the recombination processes, the neutralization of D is of particular interest. It would, in fact, be desirable to dissipate the 13.6 eV recombination energy of D isotropically as radiation. Recombination of D becomes important only below 1.5 eV. At 1.2 eV, at thermal equilibrium, the densities of D ions and neutrals are equal and the transition from full ionization to full neutralization occurs in a fraction of eV. While in collisional excitation regimes the intensities of Balmer and Lyman series decay very rapidly as a function of the quantum number n, in presence of collisional-radiative recombination the decay is much slower as the upper n levels tend to be much more populated, close to their Saha equilibrium [4]. The presence of molecules in the recombining plasma also affects the spectrum, with the $n = 3$ level that is preferentially populated after an electron capture by the molecule and subsequent dissociation. It is therefore desirable for the VUV spectrometer to be able to observe the whole Lyman series, starting from the Ly-α (121.53 nm). The wavelength resolution should also allow to well separate the Ly-γ (97.23 nm) from the strong C III emission at 97.7 nm. The issue of trapping and absorption of the lowest n transitions (Ly-α and β) [5] suggest that simultaneous measurement of the Balmer α line, not as affected by radiation transport processes, should be made available for the same Lines of Sight (LOS) by means of a visible spectrometer. Means to extract the zero order to be fed into a visible spectrometer have been therefore foreseen, which should also satisfy the requirements for an absolute calibration of the VUV spectrometer, to be done in a few points of the spectrum via the branching ratio technique with emission lines in the visible. Recombination processes may be evidenced also on other species such as C, Ne or Ar [3, 6-8] by examining the relative intensities of lines from different ionization stages or different transition within the same ionization stage. Here too, the possibility of comparing the VUV spectrum with a visible one can be quite valuable as shown in [3] where

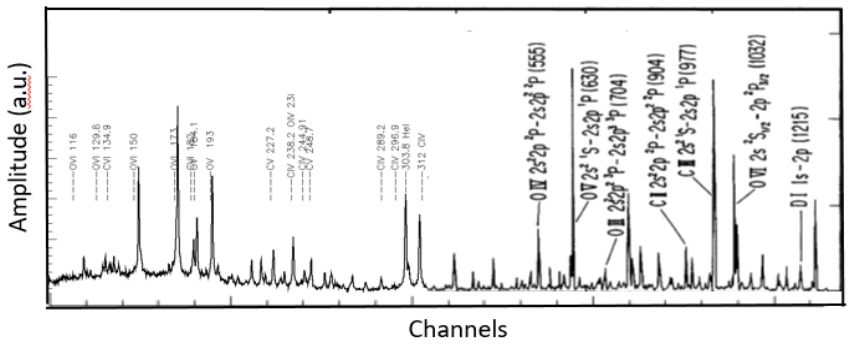

*Fig. 2. Patchwork of spectra from RFX and JT-60U [H. Kubo et al., Nucl. Fusion **33** (1993)1427] showing the expected line emission lines from the JT-60SA divertor region.*

the role of recombining vs ionizing plasma was determined using both VUV and visible C^{3+} spectra. In [9] $n = 7$ to $n = 6$ or $n = 6$ to $n = 5$ C^{3+} transitions were recognized as a signature of charge exchange recombination of C^{4+}. In this type of exercises consistency is to be sought between experimental line intensity ratios and theoretical models. Analysis of the spectra may also lead to indications on electron temperatures in the regions of the specific emission [10].

3. Spectrometer specifications

Above all it is essential that the wavelength resolution is sufficient to well resolve the emission lines of interest. In order to improve the spectral resolution a double spectrometer has been chosen. The two gratings have been selected in order to cover the two ranges 10-48 nm and 44-125 nm, with an overlapping region that includes the 45.96 nm C III line for cross calibration. Wavelength resolution is predicted to be 0.08 and 0.14 nm respectively [11]. As specified before the long wavelength range includes the Ly-α line at 121.53 nm but also the N V doublet at 1238.8/1242.8 Å. Extending the short wavelength range to 10 nm allows various metal lines to be observed. Below 10 nm the spectrometer sensitivity is expected to fall steeply. The other important consideration is that lines from a particular ionization stage fall on the same detector whenever possible, this making the analysis of these lines more reliable. The idea of focusing in particular on C^{3+} has favored the choice of the 44-48 nm overlap, also quite suitable for monitoring Ne II emission lines. Given the large contribution (90%) of the C^{3+} 154.8/155.1 nm doublet to the total C^{3+} radiated power, there is interest in measuring its intensity directly. However, given the difficulties in obtaining a spectrometer absolute sensitivity calibration at that wavelength the contribution to radiated power of C is best determined by an analysis of six of the short wavelength C^{3+} lines. An exception is in the event of a strong C influx, when the long wavelengths doublet lines, which are somewhat more sensitive to ionization than the shorter wavelength lines [10] give a better indication of the C^{3+} radiated power. However, this is likely to be an infrequent event with a modest effect. Therefore, on balance, considering the additional fact that no particular significant lines fall between the C^{3+} doublet and the Ly-α it is argued that there is more gain by having the higher spectral resolution for the long wavelength detector, whose range is therefore limited to 125 nm. The resolution of the first grating is adequate also for the later phase with W based PFCs.

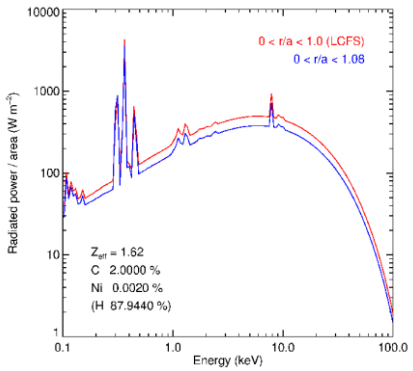

Fig. 3. The volume average power per unit area across the LCFS (red) and across the SOL (boundary of the simulation - blue) for a mixture of impurities as indicated.

Since the LOS of the spectrometer crosses vertically the plasma, an effort has started in order to predict the expected spectrally resolved emission from the main plasma. Using the background plasma and the impurity transport coefficients of previous simulations of JT-60SA plasmas [12, 13], and assuming a mixture of impurities, the steady-state radiated power per unit area across the LCFS has been calculated in the energy range between 0.1 and 100 keV. A sample result is shown in Fig. 3. Extension of the exercise below 0.1 keV, the region covered by the spectrometer, requires that the divertor region is included as the spectral emission in

the spectrometer range is quite sensitive to the details of the LOS. This will be done in the next future based on suitable EDG2D simulations. In Fig. 3 one may notice the (expected) trend of the continuum radiation, which could be used, in principle, for evaluations of Z_{eff}, provided the stray radiation in the spectrometer can be kept at adequately low levels [13].
One last consideration regards the required time resolution. Ideally the instruments should be able to resolve ELMs. Available 2D high sensitivity CCD detectors have readout schemes flexible enough to allow for repetition rates below 0.5 kHz when the readout area is significantly reduced in size. However, in imaging mode, with several spectra binned on the chip and read serially, the readout frequency will be much slower, below 10 Hz.

4. Current status of the spectrometer design

The spectrometer will be based on the double SPRED spectrometer used on Textor [15], refurbished with new gratings, specially designed following an optimization technique that maximizes the spectral resolution for the given etendue [11], and two new CCD detectors. Two mirrors inside the spectrometer will reflect the zero order out of the spectrometer for calibration purposes and also to complement the VUV spectral information with spectra collected in the visible, as mentioned above. As there is no direct view of the entire divertor from the top ports two toroidal mirrors will be placed inside the port in order to focus the divertor on to the entrance slits of the spectrometer. Alternative optical schemes are under study although the former one should provide adequate imaging quality (resolution of 7-10 cm across the divertor). In principle the alignment of spectrometer and double mirror system will be achieved making spectrometer and mirrors part of a single solid body, with adjustments to be refined in the laboratory before installation.

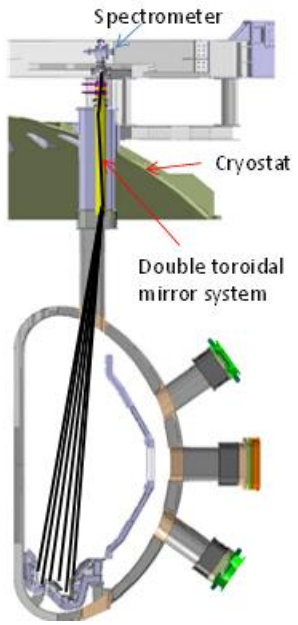

Fig. 4. Overview of the viewing geometry.

Acknowledgements: This work has been carried out within the framework of the EUROfusion Consortium and has received funding from the EURATOM research and training programme 2014-2018 and 2019-2020 under grant agreement No 633053. The views and opinions expressed herein do not necessarily reflect those of the European Commission. The authors gratefully acknowledge members of the JT-60SA Integrated Project Team for data exchange and fruitful discussions.

References

[1] JT-60SA Research Plan V4.0, http://www.jt60sa.org/pdfs/JT-60SA_Res_Plan.pdf. [2] M. Romanelli *et al.* (2017) *Nucl. Fusion* **57** 116010. [3] T. Nakano, *et al.* (2007) *Nucl. Fusion* **47** 1458. [4] R.C. Isler *et al.* (1997) *Phys. Plasmas* **4** 2989. [5] J.L. Terry *et al.* (1998) *Phys. Plasmas* **5** 1759. [6] M. Mattioli *et al.* (2002) *Plasma Phys. Control. Fusion* **44** 33. [7] T. Nakano *et al.* (2013) *J. Nucl. Mater.* **438** S291. [8] K. Lawson *et al.* (2013) *J. Phys. B* **46** 035701. [9] B. Zaniol *et al.* (2001) *Phys. Plasmas* **8** 4386. [10] K.D. Lawson *et al.* (2011) *Plasma Phys. Contr. Fusion* **53** 015002. [11] W. Biel *et al.* (2004) *Rev. Sci. Instrum.* **75** 3268. [12] R. Zagorski *et al.* (2016) *Nucl. Fusion* **56** 016018. [13] L. Garzotti *et al.* (2018) *Nucl. Fusion* **58** 026029. [14] H. Zhou *et al.* (2012) *Rev. Sci. Instrum.* **83** 10D507. [15] W. Biel *et al.* (2005) *Fusion Sci. Technol.* **47** 246.